Habitable Planet, 2025, 1(1&2):271–285

Habitable Planet

Journal Homepage: www.habitableplanetjournal.com

Laterite formation under tropical weathering: A geochemical characterization

P.K. Annie, Arunima M. Lal*, Arun J. John, G.K. Indu, P. Abhina, and A.S. Revathy

Department of Geology, University College, Trivandrum 695034, Kerala, India

ABSTRACT

Laterites are products of weathering in tropical and subtropical regions, and the prolonged chemical weathering produces thick residual profiles rich in iron and aluminium oxides. In addition to their economic importance as the principal sources of bauxite, nickel, and iron ores, they are also important proxies of paleoenvironment and climatic regimes. Here we investigate the laterite deposits of the Madayippara in Kannur district, Kerala, along the western margin of India, which define a flat topography. We applied geochemical techniques such as Chemical Index of Alteration and correlation coefficient analysis, to assess the relative weathering and lateritization processes across the selected profile. It is observed that SiO_2 and Al_2O_3 are the most abundant oxides in the samples. Fe_2O_3 values indicate strong ferruginization (lateritization) in the upper part of the profile, accompanied by a corresponding depletion in silica. In contrast, the bottom layer exhibits a lower Fe_2O_3 content and higher silica levels. The degree of lateritization systematically illustrates samples from various depths according to lateritization intensity, with even the sample from the deepest level falling within the weakly lateritized field. The Weathering Index of Parker (WIP) and Chemical Index of Alteration (CIA) suggest intense tropical weathering leading to the formation of laterites associated with gibbsite-rich layers. The correlation coefficient matrix between different major elements reveals a negative correlation between Fe and Si, consistent with the typical trend observed in high-grade laterites. Mineralogical studies confirmed the presence of kaolinite, gibbsite, goethite, hematite, and quartz, typical of mature laterite profiles. These findings highlight the impact of prolonged tropical weathering on the Madayippara landscape and contribute to a better understanding of the region's geological evolution and resource significance. Based on field evidence, we infer that the laterites at Madayippara developed over Tertiary sedimentary rocks during the post-Warkalli lateritisation cycle.

ARTICLE INFO

History:
Received Aug 03, 2025
Revised Sep 12, 2025
Accepted Sep 12, 2025

Keywords:
Laterites
Tropical weathering
Geochemistry
Clay mineralogy
Kerala

Citation:
Annie, P.K., Lal, A.M., John, A.J., Indu, G.K., Abhina, P., Revathy, A.S., 2025. Laterite formation under tropical weathering: A geochemical characterization. Habitable Planet 1(1&2), 271–285. https://doi.org/10.63335/j.hp.2025.0020.

Research highlights

- Degree of lateritization traced from samples collected at various depth levels
- Intense tropical weathering generated the laterites associated with gibbsite-rich layers
- Mature laterite profiles carry kaolinite, gibbsite, goethite, hematite, and quartz
- The laterites developed over Tertiary sedimentary rocks

*Corresponding author. Email: arunima@universitycollege.ac.in (AML)

1 Introduction

Laterite is a residual, *in-situ* weathering product formed through extended chemical alteration of various parent rocks under specific climatic conditions (Widdowson, 2009). It is typically rich in iron (Fe) and aluminium (Al), mainly due to the intensive leaching of silica and soluble bases from the parent material in hot, humid tropical and subtropical environments (Yadav and Das, 2021). The weathering process causes a residual build-up of iron and aluminium oxides, giving laterites their characteristic reddish colour and often leading to the development of hardened crusts or ferricrete layers. In some instances, high aluminium content can result in notable bauxite deposits, which are the primary ore of aluminium (Tardy, 1997). Lateritization is particularly associated with climatic regimes characterized by high rainfall and elevated temperatures, typically within the Köppen climate classification "A" zones (Thorne et al., 2012). These regions are primarily situated near the equator and include extensive areas in South America, Central Africa, Southeast Asia, and the Indian subcontinent.

Laterites are widely distributed across tropical and subtropical regions, including India, Brazil, West Africa, Southeast Asia, and the Philippines, where prolonged chemical weathering under warm and humid conditions produces thick residual profiles rich in iron and aluminium oxides. They are of great economic importance as the principal sources of bauxite, nickel, and iron ores (Giorgis et al., 2014), while also serving as paleoenvironmental archives that record ancient tropical weathering and climatic regimes (Ghosh and Guchhait, 2015; Budihal and Pujar, 2018). Regional examples highlight their dual significance: nickel laterites in Zambales, Philippines, demonstrate the role of goethite ageing and garnierite mineralization in ore potential (Aquino et al., 2022), and cobalt–nickel enriched laterites in the Piauí Province of Brazil reveal the influence of intense leaching and secondary enrichment in mafic–ultramafic terrains (Melfi et al., 1988). Together, these examples underscore that laterite studies are vital not only for resource geology and mineral exploration but also for reconstructing Earth-surface processes and long-term climate history.

In India, laterites are widely distributed, especially along the western coastal plains and nearby inland highlands. Significant deposits are found in Kerala, Karnataka, Goa, Maharashtra, and Odisha (Subramanian, 1978; Devaraju and Khanadali, 1993). These deposits are associated with the Deccan Traps in Maharashtra, the Eastern Ghats Mobile Belt in Odisha and Andhra Pradesh, the Chotanagpur Gneissic Complex in Jharkhand, the Precambrian Gneissic Complex in Tamil Nadu, and the Assam–Meghalaya Gneissic Complex. Significant occurrences are also present along both the eastern and western coasts. Indian laterites are notable not only for their extensive spatial distribution but also for their mineralogical diversity, which reflects the varied lithological and climatic conditions under which they form. These laterites typically develop on different parent rocks, including basaltic flows of the Deccan Traps, granites, gneisses, and sedimentary formations, with their characteristics being significantly influenced by regional geology and prevailing climatic conditions.

Laterites are important not only for their pedogenic development and geomorphological significance, but also for their substantial economic value, as significant sources of vital mineral ores, including bauxite and iron ores such as hematite and goethite (Tardy, 1997), as well as several critical metals and rare earths (Economou-Eliopoulos et al., 2021). The lateritic profile often includes a hardened ferruginous crust called "ironstone" and underlying saprolite, which varies in composition and thickness depending on factors such as climate fluctuation and parent rock chemistry (Selby, 1993).

Madayipara is a key lateritic formation in northern Kerala, located in the southern part of the Indian Peninsula, and showcases typical tropical weathering and laterite formation. Situated in Madayi village near Payangadi in Kannur district, it exemplifies a midland lateritic body in the region (Narayanaswami, 1992). The laterite profile in this region features well-developed pisolitic, massive, and vesicular textures, often resting atop lithomarge clay and bauxitic horizons, signalling advanced weathering stages. Layers of laterite, silty sandstone, sandstone, lignite, and clay are present at Madayipara. This study primarily focuses on the geochemical characterization of the laterites in this area with the objective of understanding the process of laterite formation under tropical weathering conditions.

2 Geological setting

In Kerala, laterites develop over various parent rocks, including charnockites, khondalites, and gneisses. The study examined the development of lateritic profiles in a typical locality in North Kerala, highlighting the influence of climate and lithology. Madayipara is one of the most significant lateritic exposures in northern Kerala, exhibiting the typical features of tropical weathering and laterite formation. Located in Madayi village near Payangadi town in Kannur district, it serves as a classic example of a laterite formation on the top of tertiary formation in northern Kerala. Situated between latitudes 12°01′ to 12°03′ N and longitudes 75°14′ to 75°16′ E, the exposure lies at an elevation of 30 to 70 m above sea level. It covers approximately 365 hectares (Fig. 1). The laterite outcrops in the study area have developed over the tertiary Cheruvathur formation, which acts as the parent material (Indu et al., 2025). The surface of this exposure is undulating, with a thin soil cover, exposed laterite rock, and diverse microhabitats, including rock crevices, soil patches, seasonal pools,

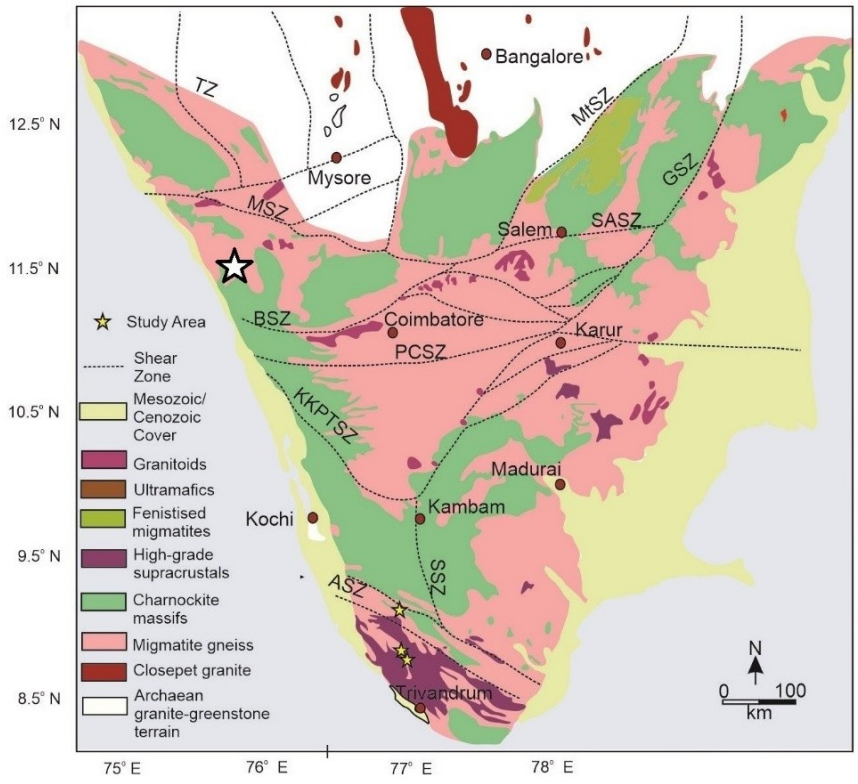

Fig. 1. Generalized geological map of southern India showing major crustal blocks and shear zones, modified from Vijaya Kumar et al. (2017).

and perennial ponds, all of which contribute to its geomorphic and ecological complexity. The laterite body represents a flat-topped erosional surface where deep weathering of the Cenozoic sediments has produced thick lateritic profiles (Fig. 2).

3 Materials and methods

To investigate the geochemical characteristics of laterites in the study area, systematic field sampling and laboratory analyses were conducted. Six samples were collected from various depths within a representative laterite profile, covering different thicknesses across the vertical section of a laterite exposure (Fig. 3 & Table 1). The sampling plan aimed to represent various textural types and degrees of weathering within the laterite profile, including hard crust, mottled zone, and soft lateritic earth. Sampling locations were identified through preliminary field reconnaissance, focusing on areas with good lateral and vertical exposure. The samples for chemical analysis were carefully cleaned to remove all debris and then air-dried at room temperature to eliminate any remaining surface moisture. All samples were ground to a fine consistency, approximately 63 µm or finer, based on texture and visual inspection, and analyzed by XRF, Central Instrumentation Facility (CIF), University of Kerala, Karyavattom. Loss on Ignition (LOI) values were determined by heating a known weight of powdered sample in a muffle furnace at 900° C for 2 h. The weight loss after heating was recorded and expressed as a percentage to calculate the LOI value. Powder X-ray diffraction (XRD) analysis was performed to determine the mineralogical composition of the laterite samples, providing insight into the degree of weathering and secondary mineral formation. The XRD analysis was conducted at the Central Instrumentation Facility (CIF), University College, Trivandrum, using a Rigaku MiniFlex Powder X-ray diffractometer.

Location	Sample identity	Bed elevation from sea level (m)	Description of sample
Location-1 Madayipara	M1	52	Laterite
	M2	49.8	
	M3	48.3	
	M4	47.8	
	M5	47.3	
	M6	46.8	

Table 1. Sample collection details with depth information.

Fig. 2. Field photographs of the study area. (A) The circle indicates the clay layer of the Cheruvathur Formation, which underlies the laterite. (B) and (D) display the pisolitic structure, while (C) illustrates the vertical section of the Madayipara laterite.

4 Results and discussion

4.1 Geochemistry

The chemical composition of lateritic samples was characterised by X-ray Fluorescence (XRF) for the major and some trace elements, and X-ray Diffraction (XRD) for mineralogical phase composition. The geochemical analysis of samples using XRF reveals distinct trends in principal oxides, reflecting progressive weathering and compositional changes across the profile. Geochemical variation of

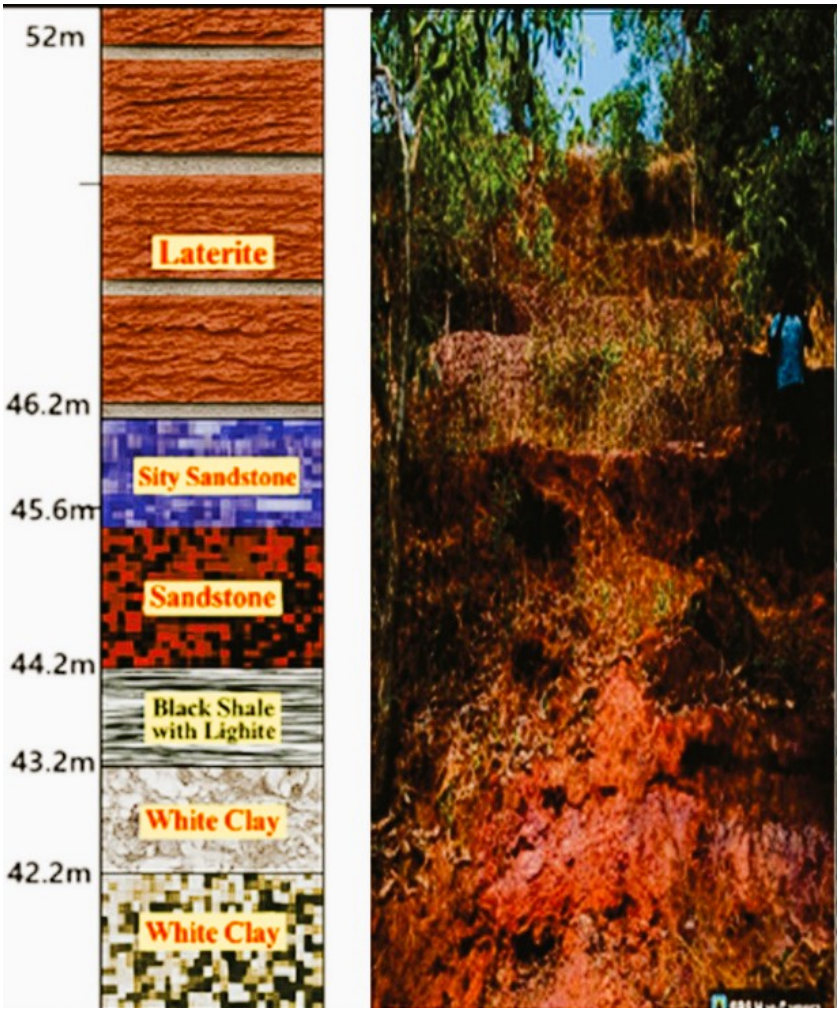

Fig. 3. Left—Stratigraphic section of Madayipara; Right—Vertical profile of the laterite.

primary elemental oxide composition in each sample is presented in Table 2. The silica content rises steadily from 9.88% in M-1 to 47.6% in M-6, marking a shift from desilicated upper layers to more siliceous lower horizons. Iron oxide shows a significant decline from 51.7% in sample M-1 to just 8.81% in M-6, suggesting strong ferruginisation in the upper sample (Fig. 4). Aluminium oxide, in contrast, increases from 27.1% in M-1 to a peak of 40.8% in M-3, followed by a slight decrease, indicating aluminium enrichment and possible bauxitization in the middle zone. Titanium dioxide remains relatively stable, with a slight enrichment in M-3, consistent with its resistance to chemical weathering. Phosphorus pentoxide gradually decreases across the samples, likely due to the leaching of associated phosphate and iron phases. Oxides of calcium, magnesium, sodium, and potassium remain low throughout, with occasional spikes, notably, K_2O peaks in M-3 reflecting the mobility of base cations under intense weathering conditions.

The geochemical trends related to weathering can be explained by scatter diagrams (Fig. 5). A slight negative correlation is observed between SiO_2 and Al_2O_3, indicating alumina enrichment in more weathered, silica-depleted samples. Similarly, TiO_2 and Fe_2O_3 both show decreasing trends with increasing SiO_2, with Fe_2O_3 displaying a strong negative correlation, suggesting iron enrichment in less siliceous zones due to laterization. P_2O_5 also decreases with rising silica, reflecting phosphorus retention in more weathered areas. In contrast, CaO shows a slight positive correlation with SiO_2, implying that calcium is more common in less altered, silica-rich parts of the profile. K_2O displays no clear trend, with scattered values possibly due to local mineralogical differences. MnO and MgO both decrease as silica increases, indicating leaching of manganese and magnesium during progressive weathering. Na_2O shows a weak positive trend, suggesting minimal retention of sodium in silica-rich zones. Overall, these patterns highlight the typical geochemical behaviour of

	M-1	M-2	M-3	M-4	M-5	M-6
Fe_2O_3	51.7	34.3	17.1	9.39	7.11	8.81
Al_2O_3	27.1	36.3	40.8	32.1	29.2	30.5
SiO_2	9.88	18.9	20.8	42.1	46.9	47.6
TiO_2	1.87	2.33	3.46	1.95	1.9	1.7
P_2O_5	0.46	0.225	0.19	0.0744	0.0556	0.0607
CaO	0.0599	0.11	0.0476	0.226	0.253	0.177
MnO	0.0294	0.0203	0.0239	0	0.0132	0.0138
SO_3	0.019	0.0246	0.0124	0.0146	0.0202	0.0132
K_2O	0.0162	0.211	0.797	0.22	0.203	0.144
MgO	0	0	0.206	0.103	0.13	0.0878
Na_2O	0	0	0	0.0735	0.0176	0.0727
LOI	10.65	10.74	19.39	13.25	11.33	11.04

Table 2. Major oxide concentrations (wt%) in the analysed samples.

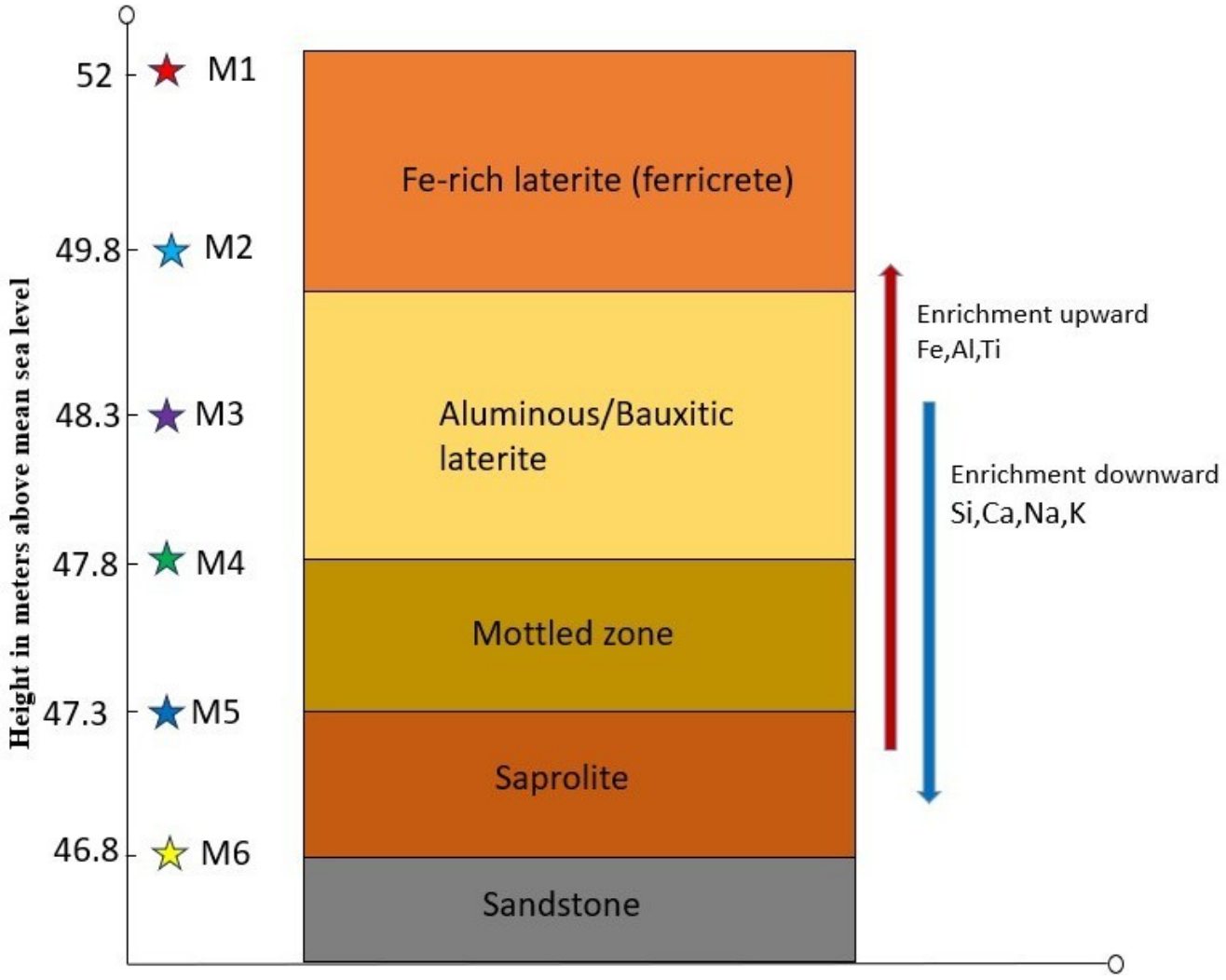

Fig. 4. Schematic diagram of the vertical profile of the laterite showing enrichment and depletion of various elements.

principal oxides during the development of laterite under tropical weathering conditions (Fig. 6).

The correlation matrix gives a clear picture of how different major elements interact during the formation of laterite

	Fe	Al	Si	Ti	P	Ca	Mn	S	K	Mg	Na
Fe	1.00	−0.16	−0.90	0.00	0.97	−0.71	0.75	0.49	−0.31	−0.72	−0.63
Al	−0.16	1.00	−0.26	0.90	−0.14	−0.43	0.11	−0.19	0.88	0.49	−0.29
Si	−0.90	−0.26	1.00	−0.44	−0.91	0.90	−0.80	−0.32	−0.14	0.39	0.77
Ti	0.00	0.90	−0.44	1.00	0.10	−0.60	0.36	−0.25	0.95	0.58	−0.51
P	0.97	−0.14	−0.91	0.10	1.00	−0.78	0.79	0.32	−0.19	−0.55	−0.65
Ca	−0.71	−0.43	0.90	−0.60	−0.78	1.00	−0.84	0.02	−0.37	0.14	0.65
Mn	0.75	0.11	−0.80	0.36	0.79	−0.84	1.00	0.24	0.13	−0.24	−0.82
S	0.49	−0.19	−0.32	−0.25	0.32	0.02	0.24	1.00	−0.46	−0.68	−0.53
K	−0.31	0.88	−0.14	0.95	−0.19	−0.37	0.13	−0.46	1.00	0.80	−0.27
Mg	−0.72	0.49	0.39	0.58	−0.55	0.14	−0.24	−0.68	0.80	1.00	0.13
Na	−0.63	−0.29	0.77	−0.51	−0.65	0.65	−0.82	−0.53	−0.27	0.13	1.00

Table 3. Correlation coefficients of principal oxides of the laterite deposits of the study area.

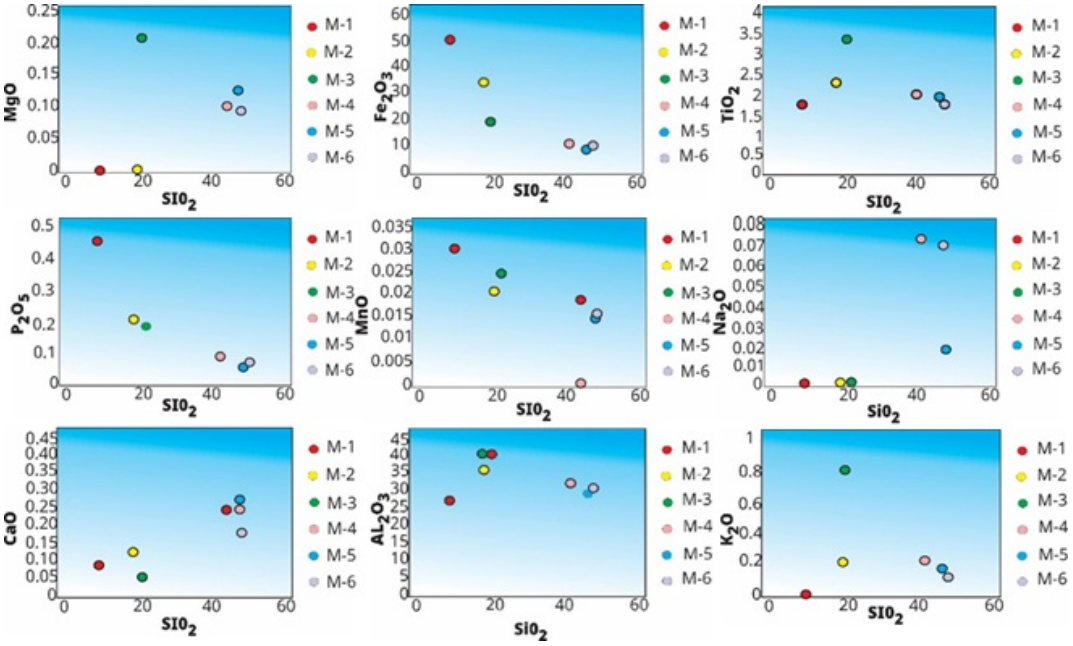

Fig. 5. Scatter plots showing variations of major oxides in the studied laterites.

in Madayipara. Iron oxide exhibits a strong positive correlation with phosphorus and manganese oxides, suggesting they are likely concentrated together in iron-rich minerals that form during weathering. Iron oxide has a strong negative correlation with silicon content, reflecting the breakdown of silicate minerals and the build-up of iron oxides, a typical trend in highly weathered soils (Wille et al., 2018). Aluminium oxide also shows an interesting pattern, being negatively related to potassium, likely due to the leaching of K-bearing minerals. At the same time, aluminium remains in stable clay minerals, such as gibbsite or kaolinite. Titanium, which is usually quite resistant to weathering, shows positive associations with Al_2O_3 and K_2O, suggesting it is tied to more stable mineral phases that remain in the soil. Elements like calcium (Ca) and sodium (Na) exhibit mostly negative relationships with others, indicating their loss during weathering (Guinoiseau et al., 2021). Overall, the matrix shows a clear divide; some elements like Fe, Al, and Ti tend to accumulate as the soil matures, while others like Ca, Na, and K are more easily washed away. This pattern is typical of how laterites form under hot, wet conditions where chemical weathering is intense (Budihal and Pujar, 2018). Pearson correlation coefficients between different major elements (Fe, Al, Si, Ti, P, Ca, Mn, S, K, Mg, Na) in the laterite samples are calculated and shown in Table 3.

During lateritization, aluminosilicate minerals undergo progressive chemical weathering under intense leaching conditions. Feldspars and micas, which are abundant in the parent rocks, are initially altered to kaolinite through hydrolysis reactions, accompanied by the release of soluble cations such as Na^+, Ca^{2+}, and K^+. With continued

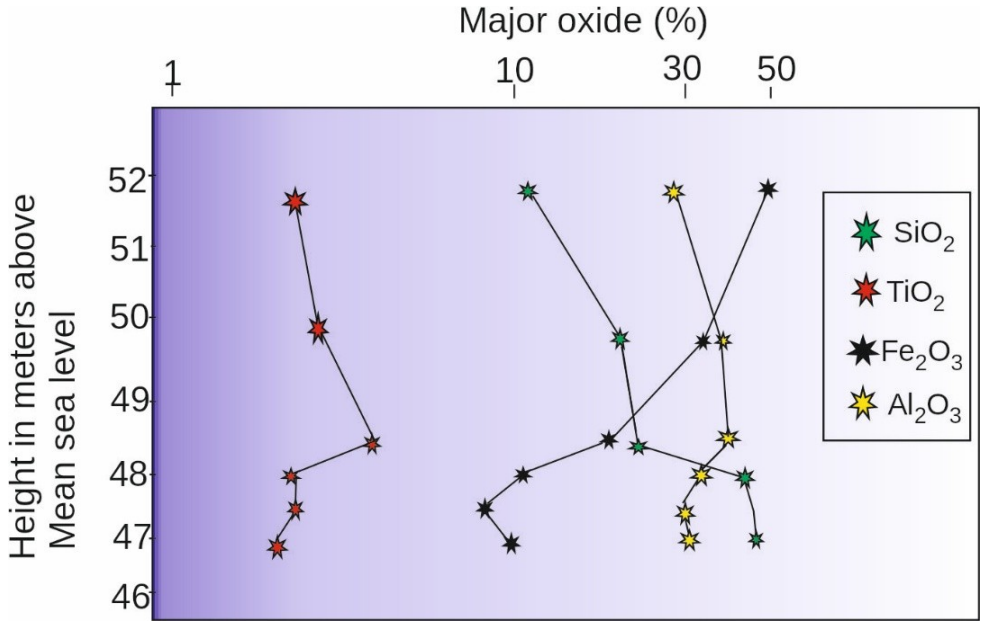

Fig. 6. Distribution patterns of major oxides across the laterite profile.

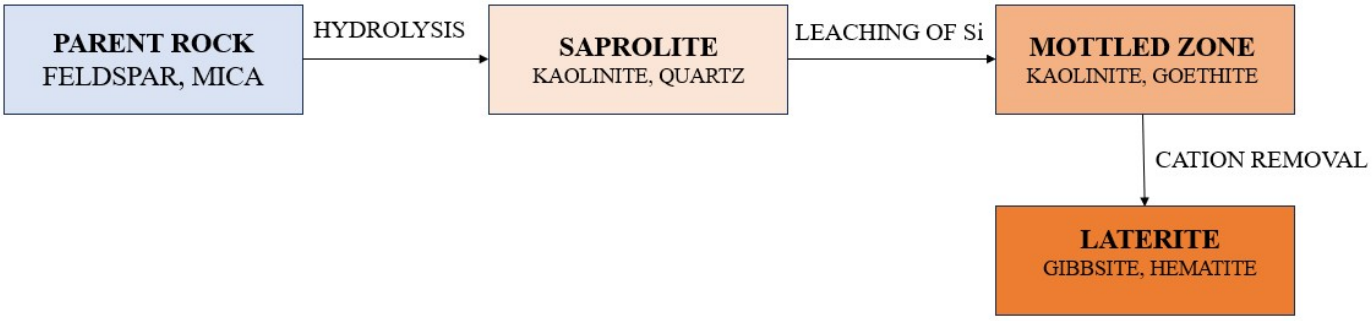

Fig. 7. Chemical seathering sequence from parent rock to laterite.

weathering, silica is progressively leached out, resulting in the relative enrichment of aluminium and the subsequent formation of gibbsite. This mineralogical transformation from feldspar $\longrightarrow$ kaolinite $\longrightarrow$ gibbsite represents a key pathway in the geochemical evolution of laterites in humid tropical climates (Parker, 1970; Nesbitt and Young, 1984; Nahon, 1991; Tardy, 1997). The accumulation of secondary aluminium hydroxides (gibbsite) is a diagnostic feature of highly mature laterite profiles (Valeton et al., 1987; Beauvais and Tardy, 1993).

4.2 Reactions involved in the formation of laterite

Laterite formation involves the progressive weathering of feldspar to kaolinite through hydrolysis, followed by silica leaching that transforms kaolinite into gibbsite under intense tropical conditions (Fig. 7).

1. Feldspar to Kaolinite (Hydrolysis)

$$2NaAlSi_3O_8 + 2H^+ + 9H_2O \longrightarrow Al_2Si_2O_5(OH)_4 + 4H_4SiO_4 + 2Na^+$$

(Albite is altered to kaolinite, releasing silica and sodium into solution.)
(Nesbitt and Young, 1984; Nahon, 1991)

2. Kaolinite to Gibbsite (silica leaching)

$$Al_2Si_2O(OH)_4 + 2H_2O \longrightarrow 2Al(OH)_3 + 2SiO_2$$

(Kaolinite undergoes desilication to form gibbsite and free silica)
(Beauvais and Tardy, 1993; Tardy, 1997)

3. Mica/Biotite to Gibbsite + Iron oxide

$$K(Mg,Fe)_3AlSi_3O_{10}(OH)_2 + H^+ + O_2 \longrightarrow Al(OH)_3 + FeO(OH) + \text{soluble ions}$$

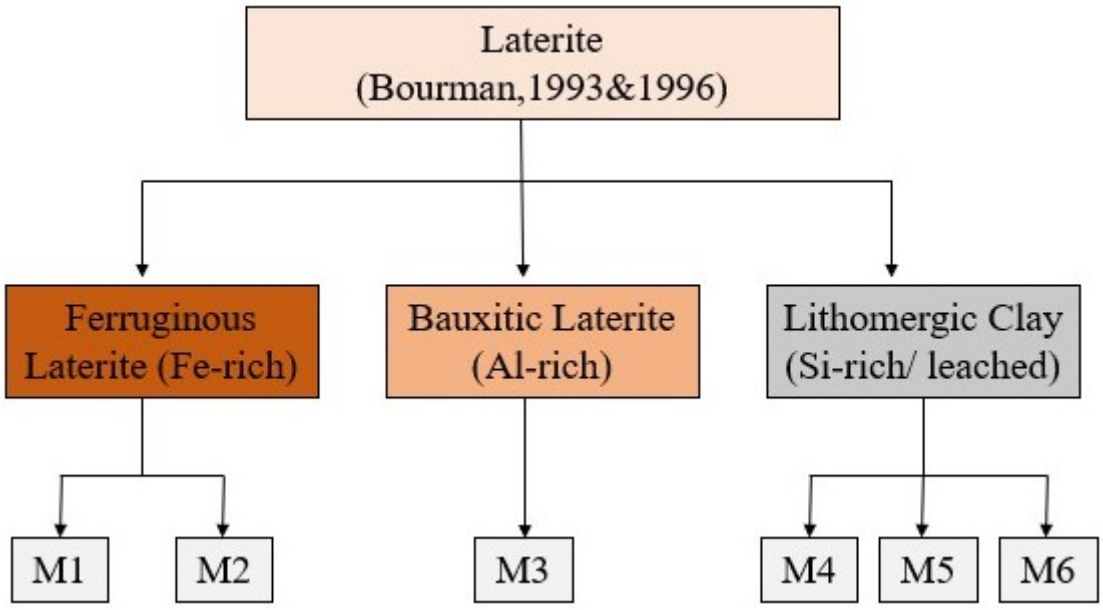

Fig. 8. Classification of Madayipara aterite after Bourman (1993, 1996).

Criteria	Classification of Madayipara laterite
Mode of occurrence	Plateau Laterite (capped hill surface)
Morphology	Massive Ferricrete with pisolitic varieties
Degree of lateritisation	Mature laterite
Profile expression	Ferruginous-aluminous laterite sequence
Age	Tertiary Laterite (Cheruvathur Formation, N Kerala)

Table 4. Classification of Madayipara laterite (after Bourman, 1993, 1996).

(Micas weather to aluminium hydroxides and secondary iron oxides such as goethite and hematite.) (Valeton et al., 1987; Nahon, 1991)

Laterites have been classified in various ways, and one widely accepted scheme is that of Bourman, who emphasized their genesis, composition, and degree of weathering. According to this classification, laterites represent a spectrum of highly weathered materials ranging from ferruginous and aluminous crusts to clay-rich saprolites. The system distinguishes between true laterites, which are hardened and often form capping profiles, and related materials, such as lateritic soils and mottled zones, that occur at intermediate stages of weathering (Bourman, 1993, 1996; Bourman and Ollier, 2002). This classification thus provides a genetic and morphological framework for understanding lateritic profiles in different geomorphic and climatic settings (Fig. 8 and Table 4).

4.3 Degree of laterization

The lateritization process observed in the study area reveals a well-defined vertical geochemical zonation, characteristic of intense chemical weathering under tropical climatic conditions. This zonation typically progresses from a silica-rich basal zone, through an aluminium-enriched middle horizon, culminating in an iron-rich upper crust. Such stratification reflects the progressive mobilization and redistribution of elements during prolonged weathering of parent rock material in a high-temperature, high-rainfall environment. At the base of the profile, the presence of elevated SiO_2 content suggests minimal leaching and preservation of primary silicate minerals (Sari et al., 2024). As weathering intensifies upwards, silica is progressively leached, while aluminium becomes concentrated in more stable secondary minerals such as gibbsite and kaolinite, resulting in an Al-rich middle zone (Nahon, 1991; Tardy, 1997). This horizon often represents the bauxitic layer, indicative of advanced desilicification. In the uppermost part of the profile, Fe-oxides such as hematite and goethite become dominant due to the accumulation of insoluble iron released from ferromagnesian minerals (Fu et al., 2014). The high Fe_2O_3 concentrations in this zone reflect both the immobility of iron under oxidizing conditions and its tendency to form coatings or concretions (Maignien, 1966;

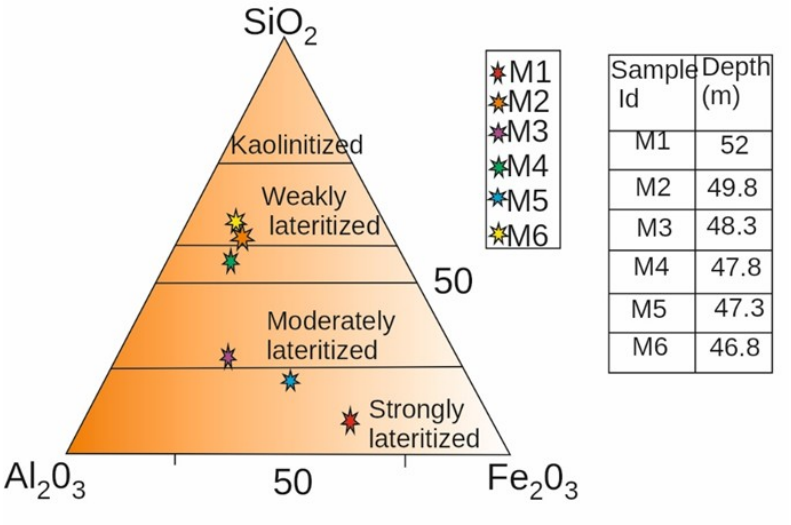

Sample Id	Depth (m)
M1	52
M2	49.8
M3	48.3
M4	47.8
M5	47.3
M6	46.8

Fig. 9. Triangular plot of SiO_2–Fe_2O_3–Al_2O_3 indicating degree of lateritization (after Schellmann, 1986). CIA = Al_2O_3/(Al_2O_3+CaO+Na_2O+K_2O) × 100.

Index	Formula	Interpretation
CIA (Chemical Index of Alteration)	$Al_2O_3/(Al_2O_3 + CaO + Na_2O + K_2O)$ ×100	<50 = weak weathering; 50–80 = moderate; >80 = intense weathering (lateritic conditions).
WIP (Weathering Index of Parker)	$(2Na_2O/0.35 + MgO/0.9 + CaO/0.7)$ ×100	>100 = Fresh rock; 60–100 = Weathered; <60 = Strongly weathered or lateritized

Table 5. The Chemical Index of Alteration (CIA) after Nesbitt and Young (1989).

Schaefer et al., 2008). This vertical differentiation is a hallmark of lateritic weathering, where element mobility is primarily governed by solubility and stability under acidic, oxidizing, and fluctuating moisture conditions. Elements such as Si, Na, K, and Ca are generally mobile and removed through leaching, whereas Fe, Al, and Ti are relatively immobile and hence enriched in the weathered residue (Yadav and Das, 2021). The observed geochemical profile at Madayipara aligns with classical models of laterite formation in tropical regions, where intense leaching leads to a residual concentration of Fe_2O_3 and Al_2O_3 (Figs. 6 and 9).

4.4 Weathering intensity

The Chemical Index of Alteration (CIA) is a widely used geochemical tool for assessing the degree of chemical weathering in rocks and soils, particularly in lateritic and tropical weathering environments. CIA is interpreted as a measure of the extent of feldspar conversion to clays (Nesbitt and Young, 1989; Fedo et al., 1995). It quantifies the removal of mobile elements (Ca, Na, K) during chemical weathering, providing insights into the intensity of alteration and the paleoclimatic conditions under which the weathering occurred.

CIA values often range from 85 to 100, indicating intense tropical weathering and leaching of mobile elements (Ca, Na, K). A value close to 100 suggests extreme weathering, often associated with bauxite or gibbsite-rich laterite (Nesbitt and Young, 1984). The values of the Chemical Index of Alteration (CIA) for all six samples are very high, ranging from 96.04 to 99.51. These values suggest the samples have undergone intense chemical weathering. The highest CIA value is observed in sample M-1, which exhibits the most extreme alteration, while sample M-3 has the lowest, yet still clearly reflects heavy weathering. The intensity of chemical weathering is evaluated by the Weathering Index of Parker (WIP). Unlike the Chemical Index of Alteration (CIA), which focuses mainly on alumina and alkali/alkaline earth elements, the WIP incorporates a weighted molar ratio of mobile base cations relative to their susceptibility to weathering (Nadłonek and Bojakowska, 2018). This index is particularly useful in understanding element mobility during the weathering process and in assessing the residual enrichment or depletion of major cations, such as Ca, Na, K, and Mg.

$$WIP = 100\times (2Na_2O/0.35+MgO/0.9+2K_2O/\ 0.25+CaO/0.7)$$

The WIP values less than 20 suggest intense tropical weathering leads to the formation of laterites. The Weathering Index of Parker (WIP) adds more detail to this picture. All the samples have very low WIP values, ranging from

0.24 to 4.07, which is consistent with advanced weathering and the near-total removal of base cations. These low values confirm that the material has been strongly leached over time. The trend also shows that as CIA values increase, WIP values tend to decrease, which makes sense, since one measures what is left behind (like aluminum) and the other reflects what has been lost (like calcium and sodium). Together, the CIA and WIP results tell a clear story: all six samples come from a deeply weathered laterite profile, where long-term chemical processes have reshaped the original rock into a highly altered and mature soil material.

5 6 XRD analysis

Mineral identifications were made by comparing observed 2θ and d-spacing values with the Xpert High Score Plus software, Match Software, and also by using where peak positions and intensities were matched against reference patterns from the ICDD PDF-4+ database, RRUFF database, and supported by standard references such as Jeans et al. (1997) and Brindley and Brown (1980). This facilitated accurate identification of key minerals typically found in lateritic materials, such as kaolinite, gibbsite, hematite, goethite, and quartz.

The XRD analysis of the six laterite samples (M-1 to M-6) revealed a typical mineral composition associated with strongly weathered tropical soils. Kaolinite was the most prominent mineral across all samples, as indicated by firm diffraction peaks around 12.3° to 12.5° 2θ and near 25°, which are characteristic of its crystal structure (Brindley and Brown, 1980) (Fig. 10). The widespread presence of kaolinite suggests that the samples have undergone prolonged chemical weathering in warm and humid conditions ideal for the breakdown of primary silicate minerals (Keller, 1956). Alongside kaolinite, Gibbsite was also consistently detected, particularly between 14° and 21° 2θ. This aluminium-rich mineral typically forms in lateritic profiles during intense leaching, where silica is removed and aluminium becomes concentrated. Another key phase identified in the samples was Quartz, showing a sharp and distinctive peak at around 26.7° 2θ, along with multiple peaks at higher angles. Quartz is a highly resistant mineral that often remains after other components have been weathered away (Wilson, 2020). Its presence indicates a residual or detrital origin, suggesting contributions from the original parent rock or external inputs. In addition, all six samples exhibited peaks corresponding to Goethite and Hematite, two iron oxide minerals that commonly form in lateritic environments. Peaks between 33° and 42° confirmed their presence, with hematite indicating more oxidizing, drier conditions, while goethite suggests slightly more hydrated environments. These minerals are primarily responsible for the reddish-brown coloration typical of laterite soils. A few smaller peaks also indicated the presence of Anatase (TiO_2) in all samples. Although not a primary phase, anatase is significant because it tends to form during intense weathering and remains stable over long periods. Its presence further supports the conclusion that these samples are from a mature lateritic profile. XRD data imply an intense tropical weathering, resulting in a stable mineral assemblage dominated by kaolinite, gibbsite, quartz, hematite, goethite, and anatase. These findings align well with the typical mineralogical signature of laterite and provide strong evidence for advanced weathering, leaching, and residual enrichment in the studied area.

6 Discussion and conclusion

The geochemical study of the laterite in Madayippara in North Kerala illuminates the nature of weathering and the parent rock, involving tracing the origin and history of lateritization. The laterite profile overlies Tertiary formations consisting of sandy, clayey, and lignite-rich layers, indicating a complex weathering history influenced by both lithology and climate. The development of laterite above these formations is mainly attributed to intense chemical weathering under tropical climatic conditions characterized by high rainfall, high temperatures, and prolonged wet-dry cycles. These conditions promote the leaching of silica and mobile bases from the parent sedimentary rocks, leading to the enrichment of iron and aluminum oxides. It is observed that SiO_2 and Al_2O_3 are the most abundant oxides in the samples. Fe_2O_3 values suggest strong ferruginization (lateritization) in the upper part of the profile. Laterites in the district have formed through two distinct cycles of lateritization—one over the Precambrian basement and the other over the Tertiary formations. Geochemical trends support *in situ* field evidence, indicating that the laterites at Madayippara developed over Tertiary sedimentary rocks during the post-Warkalli lateritization cycle. The top layer shows enrichment in Fe_2O_3 and a corresponding depletion in silica, while the bottom layer exhibits lower Fe_2O_3 content and higher silica levels. This geochemical trend suggests that the laterite profile has developed over Tertiary sedimentary parent material. Geomorphologically, the region features elevated, laterite-capped undulating terrain, which promotes efficient surface drainage and prolonged exposure of sediments to weathering agents. The presence of underlying sandy and lignite-bearing layers indicates that lateritization occurred after deposition, modifying the Tertiary sequences *in situ*. The lignite layers suggest a prior swampy environment, which, upon uplift and exposure, transitioned into a lateritic weathering regime.

The correlation coefficient matrix between different major elements indicates a negative correlation between Fe and Si, reflecting the breakdown of silicate minerals and the build-up of iron oxides, a typical trend in highly weath-

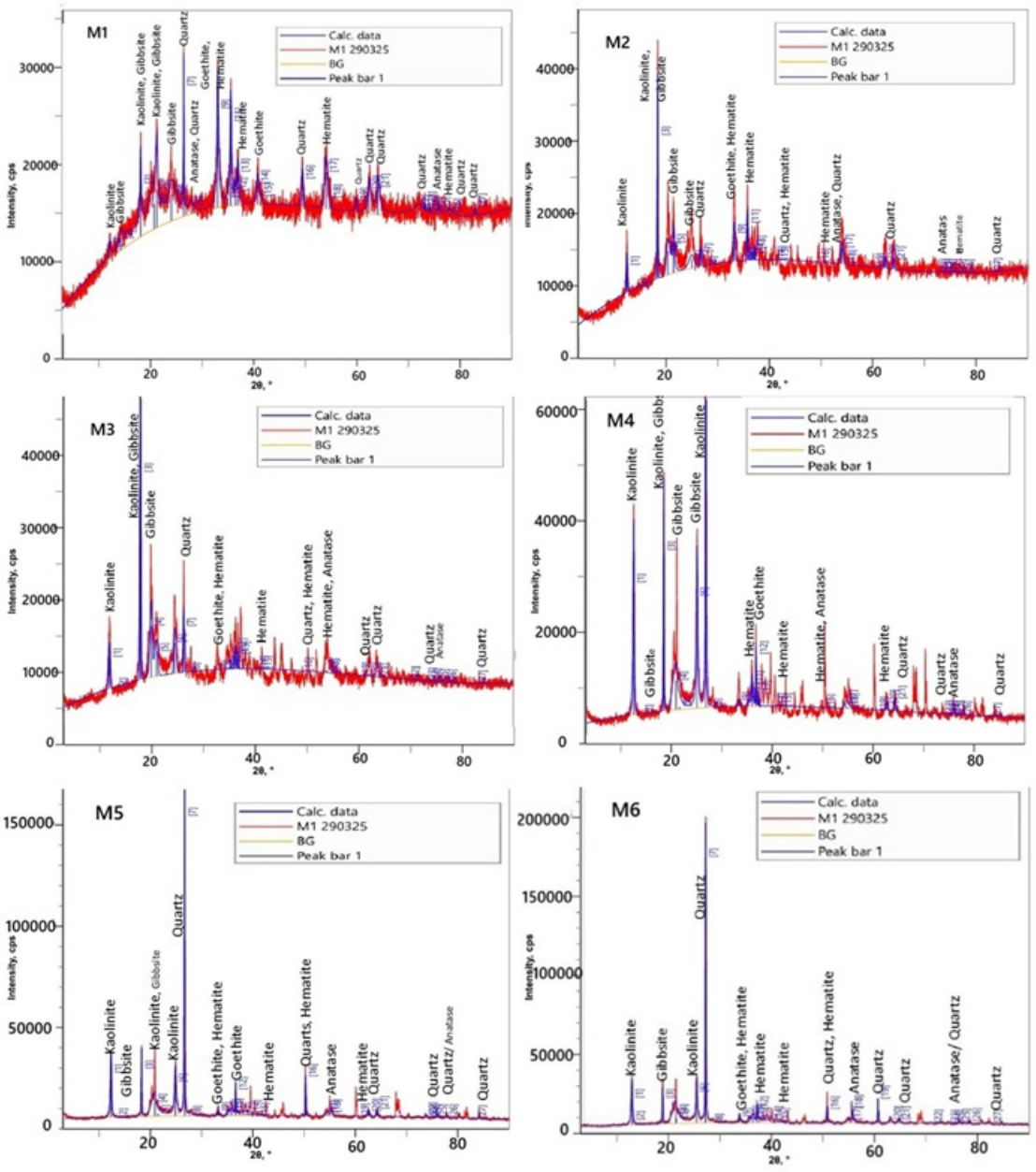

Fig. 10. XRD peak of M-1, M-2, M-3, M-4, M-5 and M-6 sections of laterite in the study area.

ered soils (high-grade laterites). In lateritic profiles, a clear geochemical pattern often appears as a reverse correlation between Fe and Si, indicating intense chemical weathering in tropical environments. During the lateritization process, silicon, primarily found in silicate minerals such as quartz and feldspar, is gradually leached out due to its higher solubility in humid conditions. Conversely, iron tends to become less mobile, accumulating as oxides such as hematite and goethite, leading to Fe enrichment in areas where Si has been depleted. This inverse relationship indicates advanced desilicification and the maturity of lateritic stages. High Al_2O_3 concentrations are observed at M3, likely due to the relative immobility of aluminium during weathering. As silica is leached and iron becomes less mobile at depth, aluminium accumulates as gibbsite or kaolinite, especially in zones derived from feldspar- or mica-rich parent rocks. This results in the formation of a bauxitic horizon, signifying deep weathering and mineral reconstitution under tropical climatic conditions (Table 6). Such geochemical zoning not only reflects the progression of weathering intensity but also assists in interpreting the evolution and maturity of laterite profiles. The degree of

Index / Ratio	Formula	Laterite from the study area
CIA (Chemical Index of Alteration)	$Al_2O_3/(Al_2O_3 + CaO + Na_2O + K_2O) \times 100$	The values of the Chemical Index of Alteration (CIA) for all six samples are very high, ranging from 96.04 to 99.51. These values suggest the samples have undergone intense chemical weathering.
WIP (Weathering Index of Parker)	$(2Na_2O / 0.35 + MgO / 0.9 + CaO / 0.7) \times 100$	All the samples have very low WIP values, ranging from 0.24 to 4.07, which is consistent with advanced weathering and the near-total removal of base cations. These low values confirm that the material has been strongly leached over time.
XRD		The XRD analysis of the six laterite samples (M-1 to M-6) shows dominant kaolinite and gibbsite, indicating intense chemical weathering and silica leaching under warm, humid tropical conditions.
SiO_2–Al_2O_3	SiO_2–Al_2O_3	A slight negative correlation is observed between SiO_2 and Al_2O_3, indicating alumina enrichment in more weathered, silica-depleted samples.
Fe_2O_3–Al_2O_3	Fe_2O_3–Al_2O_3	SiO_2 and Fe_2O_3 exhibit a strong negative correlation, indicating that lateritization leads to iron enrichment in zones with reduced silica content.
CaO–SiO_2	CaO–SiO_2	CaO exhibits a weak positive correlation with SiO_2, suggesting that calcium is retained mainly in the less weathered, silica-rich sections of the profile.
Geochemical Matrix		The geochemical matrix indicates that laterite formation under intense tropical weathering involves the enrichment of Fe, Al, and Ti, alongside the leaching of Ca, Na, and K.

Table 6. Key geochemical ratios with their formulas and interpretive meaning of Madayipara laterite.

lateritization plot (SiO_2–Al_2O_3–Fe_2O_3 plot) systematically illustrates samples from various depths according to lateritization intensity, with even the lowest sample falling within the weakly lateritized field. The Weathering Index of Parker (WIP) and Chemical Index of Alteration (CIA) suggest intense tropical weathering leading to the formation of laterites associated with gibbsite-rich deposits. The clay minerals identified at the Madayippara Laterite section include well-developed kaolinite, as indicated by XRD. The laterites are primarily composed of hematite, kaolinite, gibbsite, and quartz.

Lateritic weathering profiles worldwide exhibit remarkably similar mineralogical and geochemical trends, reflecting intense chemical weathering under warm, humid conditions. Studies of the Maojun Fe–Mn deposit in China show complex assemblages dominated by poorly crystalline goethite, hematite, kaolinite, illite, quartz, and minor Mn oxides, with Al_2O_3 commonly incorporated and strong negative correlations between Fe_2O_3/MnO and SiO_2 indicating progressive silica leaching (Zhao et al., 2024). In southwestern Nigeria, granite-derived profiles reveal SiO_2 depletion in the weathering horizon, enrichment of Al_2O_3 in laterite, and strong Fe_2O_3 accumulation, alongside pronounced leaching of mobile elements such as CaO, Na_2O, K_2O, P_2O_5, and MnO, consistent with intense lateritization (Adeola et al., 2017). Similarly, Permian–Triassic bauxitic-lateritic horizons in Iran are enriched in Al_2O_3 (up to 31.5%) and Fe_2O_3 (up to 37.9%), with trace and rare element patterns and high CIA, CIW, and PIA values (>80) confirming deep to moderate weathering (Abasaghi et al., 2023). In Cameroon, high rainfall and slope-dominated morphology promote silica leaching and desilicification, with mobile elements (Na, K, Ca, Mn, Mg) removed, while Al, Fe, Si, and Ti persist due to high ionic potentials, and the hardness of the duricrust increases with iron-bearing phases like goethite and hematite (Ngueumdjo et al., 2020). At Alibaltalu, residual profiles show that distributions of Si and Al are controlled by kaolinite, Ti correlates closely with Al, and Fe fractionation reflects ferruginization–deferruginization, with minor element variability influenced by protolith heterogeneity and varying alteration intensity (Abedini et al., 2023). These global observations are broadly consistent with the Madayipara laterites, which similarly exhibit dominant kaolinite and gibbsite, enrichment in Al_2O_3 and Fe_2O_3, silica leaching, and oxide ratio patterns indicative of advanced chemical weathering and lateritization processes.

Acknowledgements

The authors sincerely thank our mentor, Prof. M. Santosh, for generously spending his valuable time and providing constructive suggestions that not only improved the manuscript but also strengthened its scientific rigor. We are also grateful to Prof. Cheng-Xue Yang (Editor-in-Chief) and the anonymous reviewers for their thoughtful comments and critical insights during the review process, which greatly enhanced the overall quality and presentation of this paper. We also acknowledge the Central Instrumentation Facility (CIF), University of Kerala, Karyavattom, and UC-SAIF (University College, Thiruvananthapuram) for providing XRF and XRD analysis facilities, respectively. The authors are deeply grateful to Sri. Rajesh S., Director, GSI, SU: Kerala & Lakshadweep, and Sri. Binusarma P. E., Superintendent Geologist, GSI, SU: Kerala & Lakshadweep, for their valuable guidance during field work. We also sincerely thank Mr. Prabeesh J., Laboratory Assistant, Department of Geology, University College, Trivandrum, for his kind support and assistance with the laboratory procedures.

Declaration of completing interest

The authors declare that they have no known competing financial interests or personal relationships that could have appeared to influence the work reported in this paper.

Credit authorship contribution statement

P.K. Annie: Writing—original draft. Formal analysis, Methodology, Data curation, Resources, Software, Validation, Visualization.

Arunima M. Lal: Conceptualization, Investigation, Project administration, Supervision, Methodology, Writing—review & editing, Resources

Arun J. John: Conceptualization, Investigation, Project administration, Methodology, Supervision, Writing—review & editing

G.K. Indu: Conceptualization, Data curation, Investigation, Methodology, Supervision, Project administration

P. Abhina: Formal analysis, Methodology, Resources,

A.S. Revathy: Formal analysis, Methodology, Resources,

References

Abasaghi, F., Mahboubi, A., Mahmudi Gharaie, M.H., Khanehbad, M., 2023. Mineralogy and geochemistry of Permian–Triassic lateritic-bauxitic horizons, eastern and central Alborz, Iran: implications for provenance, palaeogeography, and palaeoclimate. Geological Journal 58(1), 170–194. doi:10.1002/gj.4585.

Abedini, A., Calagari, A.A., Mikaeili, K., 2023. Geochemical characteristics of laterites: the Ailibaltalu deposit, Iran. Bulletin of the Mineral Research and Exploration 2014(148). Article no 5. URL: https://bmta.researchcommons.org/journal/vol2014/iss148/5, doi:10.19111/bmre.55769.

Adeola, A.J., Dada, R.G., 2017. Mineralogical and geochemical trends in lateritic weathering profiles on basement rocks in Awa-Oruijebu and its environ, Southwestern Nigeria. Global Journal of Geological Sciences 15, 1–11. doi:10.4314/gjgs.v15i1.1.

Aquino, K.A., Arcilla, C.A., Schardt, C., Tupaz, C.A.J., 2022. Mineralogical and geochemical characterization of the Sta. Cruz nickel laterite deposit, Zambales, Philippines. Minerals 12(3), 305. doi:10.3390/min12030305.

Beauvais, A., Tardy, Y., 1993. Degradation and dismantling of iron crusts under climatic changes in Central Africa. Chemical Geology 107(3–4), 277–280. doi:10.1016/0009-2541(93)90190-T.

Bourman, R.P., 1993. Perennial problems in the study of laterite: a review. Australian Journal of Earth Sciences 40(4), 387–401.

Bourman, R.P., 1996. Towards distinguishing transported and in situ ferricretes: data from southern Australia. AGSO Journal of Australian Geology and Geophysics 16, 231–241.

Bourman, R.P., Ollier, C.D., 2002. A critique of the Schellmann definition and classification of 'laterite'. CATENA 47(2), 117–131. doi:10.1016/S0341-8162(01)00178-3.

Brindley, G.W., Brown, G. (Eds.), 1980. Crystal structures of clay minerals and their X-ray identification. Mineralogical Society, London. doi:10.1180/mono-5.

Budihal, R., Pujar, G., 2018. Major and trace elements geochemistry of laterites from the Swarnagadde Plateau, Uttar Kannada District, Karnataka, India. Journal of Geosciences and Geomatics 6(1), 12–20. doi:10.12691/jgg-6-1-2.

Devaraju, T.C., Khanadali, S.D., 1993. Lateritic bauxite profiles of southwestern and southern India—characteristics and tectonic significance. Current Science 64(12), 919–921. URL: https://www.jstor.org/stable/24096209.

Economou-Eliopoulos, M., Laskou, M., Eliopoulos, D.G., Megremi, I., Kalatha, S., Eliopoulos, G.D., 2021. Origin of critical metals in Fe–Ni laterites from the Balkan Peninsula: opportunities and environmental risk. Minerals 11(9), 1009. doi:10.3390/min11091009.

Fedo, C.M., Nesbitt, H.W., Young, G.M., 1995. Unraveling the effects of potassium metasomatism in sedimentary rocks and paleosols, with implications for paleoweathering conditions and provenance. Geology 23(10), 921–924. doi:10.1130/0091-7613(1995)023.

Fu, W., Yang, J., Yang, M., Pang, B., Liu, X., Niu, H., Huang, X., 2014. Mineralogical and geochemical characteristics of a serpentinite-derived laterite profile from East Sulawesi, Indonesia: implications for the lateritization process and Ni supergene enrichment in the tropical rainforest. Journal of Asian Earth Sciences 93, 74–88. doi:10.1016/j.jseaes.2014.06.030.

Ghosh, S., Guchhait, S.K., 2015. Characterization and evolution of primary and secondary laterites in northwestern Bengal Basin, West Bengal, India. Journal of Palaeogeography 4(2), 203–230. doi:10.3724/SP.J.1261.2015.00074.

Giorgis, I., Bonetto, S., Giustetto, R., Lawane, A., Pantet, A., Rossetti, P., Thomassin, J.-H., Vinai, R., 2014. The lateritic profile of Balkouin, Burkina Faso: geochemistry, mineralogy and genesis. Journal of African Earth Sciences 90, 31–48. doi:10.1016/j.jafrearsci.2013.11.006.

Guinoiseau, D., Fekiacova, Z., Allard, T., Druhan, J.L., Balan, E., Bouchez, J., 2021. Tropical weathering history recorded in the silicon isotopes of lateritic weathering profiles. Geophysical Research Letters 48, e2021GL092957. doi:10.1029/2021GL092957.

Indu, G.K., John, A.J., Lal, A.M., Anjana, R., Amrutha, K., Athulya, R., 2025. Provenance and paleoenvironmental dynamics of the Cheruvathur Formation in Northern Kerala, India: geological and geochemical perspectives. Arabian Journal of Geosciences 18, 168. doi:10.1007/s12517-025-12309-y.

Jeans, C.V., Moore, D.M., Reynolds, Jr, R.C., 1997. X-ray diffraction and the identification and analysis of clay minerals. 2nd ed., Oxford University Press, Oxford and New York.

Keller, W.D., 1956. Clay minerals as influenced by environments of

their formation. AAPG Bulletin 40(11), 2689–2710. doi:10.1306/5CEAE5CE-16BB-11D7-8645000102C1865D.

Maignien, R., 1966. Review of research on laterites (Natural Resources Research, No. 19). UNESCO, Paris.

Melfi, A.J., Trescases, J.-J., Carvalho, A., de Oliveira, S.M.B., Ribeiro Filho, E., Formoso, M.L.L., 1988. The lateritic ore deposits of Brazil. Sciences Geologiques - Bulletin 41(1), 5–36.

Nadłonek, W., Bojakowska, I., 2018. Variability of chemical weathering indices in modern sediments of the Vistula and Odra Rivers (Poland). Applied Ecology and Environmental Research 16(3), 2453–2473. doi:10.15666/aeer/1603_24532473.

Nahon, D.B., 1991. Introduction to the petrology of soils and chemical weathering. John Wiley & Sons, New York.

Narayanaswami, M.S., 1992. Geochemistry and genesis of laterite in parts of Cannanore District, North Kerala. Ph.d. thesis. Cochin University of Science and Technology. Kochi, India.

Nesbitt, H.W., Young, G.M., 1984. Prediction of some weathering trends of plutonic and volcanic rocks based on thermodynamic and kinetic considerations. Geochimica et Cosmochimica Acta 48(7), 1523–1534. doi:10.1016/0016-7037(84)90408-3.

Nesbitt, H.W., Young, G.M., 1989. Formation and diagenesis of weathering profiles. The Journal of Geology 97(2), 129–147. doi:10.1086/629290.

Ngueumdjo, Y., Wouatong, A.S.L., Ngapgue, F., et al. 2020. A petrographic, mineralogical, and geochemical characterizations of the lateritic hardpans of Bamendjou in the western region of Cameroon. SN Applied Sciences 2, 1481. doi:10.1007/s42452-020-3131-3.

Parker, A., 1970. An index of weathering for silicate rocks. Geological Magazine 107(6), 501–504. doi:10.1017/S0016756800058581.

Sari, D.V., Wibowo, G.S., Nurdiyansyah, A., 2024. Bedrock characterization and geochemical evolution of whole-rock weathering profile at GAG Ni laterite deposit, Southwest Papua, Indonesia. IOP Conference Series: Earth and Environmental Science, 1422, 012002. doi:10.1088/1755-1315/1422/1/012002.

Schaefer, C.E.G.R., Fabris, J.D., Ker, J.C., 2008. Minerals in the clay fraction of Brazilian Latosols (Oxisols): a review. Clay Minerals 43(1), 137–154. doi:10.1180/claymin.2008.043.1.11.

Schellmann, W., 1986. A new definition of laterite. Lateritisation Processes, IGCP-127. Geological Survey of India, Memoirs 120, 1–7.

Selby, M.J., 1993. Hillslope materials and processes. 2nd ed., Oxford University Press, Oxford.

Subramanian, K.S., 1978. How old are laterites in the Indian Peninsula? – A suggestion. Journal of the Geological Society of India 19(6), 269–272. doi:10.17491/jgsi/1978/190606.

Tardy, Y., 1997. Petrology of Laterites and Tropical Soils. A.A. Balkema / CRC Press, Rotterdam.

Thorne, R., Roberts, S., Herrington, R., 2012. Climate change and the formation of nickel laterite deposits. Geology 40(4), 331–334. doi:10.1130/G32549.1.

Valeton, I., Biermann, M., Reche, R., Rosenberg, F., 1987. Genesis of nickel laterites and bauxites in Greece during the Jurassic and Cretaceous, and their relation to ultrabasic parent rocks. Ore Geology Reviews 2(3), 359–404. doi:10.1016/0169-1368(87)90011-4.

Vijaya Kumar, T., Rao, Y.B., Plavsa, D., Collins, A.S., Tomson, J.K., Gopal, B.V., Babu, E.V.S.S.K., 2017. Zircon U-Pb ages and Hf isotopic systematics of charnockite gneisses from the Ediacaran–Cambrian high-grade metamorphic terranes, southern India: constraints on crust formation, recycling, and Gondwana correlations. GSA Bulletin 129(5–6), 625–648.

Widdowson, M., 2009. Laterite, in: Gornitz, V. (Ed.), Encyclopedia of Paleoclimatology and Ancient Environments. Encyclopedia of Earth Sciences Series. Springer, Dordrecht. doi:10.1007/978-1-4020-4411-3_127.

Wille, M., Babechuk, M.G., Kleinhanns, I.C., Stegmaier, J., Suhr, N., Widdowson, M., Kamber, B.S., Schoenberg, R., 2018. Silicon and chromium stable isotopic systematics during basalt weathering and lateritisation: a comparison of variably weathered basalt profiles in the Deccan Traps, India. Geoderma 314, 190–204. doi:10.1016/j.geoderma.2017.10.051.

Wilson, M.J., 2020. Dissolution and formation of quartz in soil environments: a review. Soil Science Annual 71(2), 99–110. doi:10.37501/soilsa/122398.

Yadav, P.K., Das, M., 2021. Geology, structure and geochemical features of the laterites with anomalous Ti-V-Cr and REE of the Dhandraul Formation of the Vindhyan Supergroup, Eastern India. Journal of the Geological Society of India 97(6), 603–614. doi:10.1007/s12594-021-1735-x.

Zhao, L., Niu, S., Zhou, S., Li, L., Huang, F., Wang, Y., Niu, X., Chen, T., Mo, L., Zhang, M., 2024. New insight into genesis of the Maojun laterite Fe–Mn deposit in the Lanshan area, Hunan Province, South China: evidence from detailed mineralogical and geochemical studies. Ore Geology Reviews 165, 105900. doi:10.1016/j.oregeorev.2024.105900.